Fabrication of large-area two-dimensional array of air holes with different hole shapes for optical and terahertz wavelength regions

Raj Patil,[a] **Sheng Lan,**[b] **and Achanta Venu Gopal**[a]

[a]Tata Institute of Fundamental Research, Department of Condensed Matter Physics and Material Science, Homi Bhabha Road, Mumbai 400005, India

achanta@tifr.res.in

[b]South China Normal University, School of Information and Optoelectronic Science and Engineering, Laboratory of Nanophotonic Functional Materials and Devices, Guangzhou 510006, China

Abstract. Fabrication of metal-dielectric nanostructures with subwavelength precision is necessary for plasmon-mediated novel applications. Electron beam lithography (EBL) offers such precision, but for shapes other than circles, squares, and lines, process optimization is required. The EBL and dry etching processes are optimized for subwavelength precision in large area arrays of air groove patterns in gold film in two different length scales. We fabricated one structure for optical frequencies with an asymmetric, nonstandard element having a minimum feature size of about 50 nm and another for terahertz wavelength region with a large aspect ratio of about 975. © *2014 Society of Photo-Optical Instrumentation Engineers (SPIE)* [DOI: 10.1117/1.JNP.8.083896]

Keywords: plasmonic crystals; large aspect ratio air groove arrays; electron beam lithography; metamaterials.

Paper 13090SS received Oct. 5, 2013; revised manuscript received Nov. 25, 2013; accepted for publication Dec. 10, 2013; published online Jan. 21, 2014.

1 Introduction

Plasmonic crystals, which are periodic metal-dielectric structures, are interesting for various basic physics and applied research. For example, the plasmon-mediated enhanced transmission, local field enhancement-mediated modification of linear and nonlinear optical properties, applications related to improving device performance, sensing, spectroscopy, and nanophotonics among others are some of the hotly pursued areas.[1–11]

Two plasmonic crystals are realized for specific applications in optical and terahertz (THz) wavelength regions, respectively. First structure has an array of H-shaped air grooves in gold which makes use of the shape anisotropy-based polarization-dependent response for polarization-selective switching.[12] In such a structure, the linear x- and y-polarized light have different resonances based on the dimensions of the constituent element (which is "H" in the present case). The designed structure is shown to have a good polarization selection or for a given linear polarization, the orientation of the sample controls the transmission resonance.[12]

Similarly, an array of U-shaped groove is studied for THz localization.[13] One of the ways to generate THz wavelengths is by a short-laser pulse excitation of an antenna or a nonlinear optical crystal. These processes generate broadband THz from which filtering required wavelengths is a challenging task. It was recently found that arrays of U-shaped grooves and the split ring resonators offer THz localization.[13]

In both the applications discussed earlier, fabrication is critical as the response of the structure for the desired application critically depends on the shape and quality of the pattern fabricated. Present day lithographic techniques facilitate writing structures over large areas needed for optical probing. Depending on the overall size and the minimum feature size in the pattern, there are

0091-3286/2014/$25.00 © 2014 SPIE

several techniques like direct laser writing by scanning an intense laser beam,[14] techniques based on two-photon polymerization,[15] focused ion beam,[16] nanoimprint-,[17] interference-,[18,19] and photo-[20] lithography among others.

We use electron beam lithography (EBL) for writing as it offers very high precision followed by dry etching of metal. For large area writing of arrays of asymmetric structures with large aspect ratio, several factors are to be considered. For example, stitching errors (alignment of write fields),[21] and proximity effects (effect of electron beam dose at one point depends on the dose applied at neighboring points)[21–23] among others are crucial. The novelty of this paper is in the fabrication of arrays of asymmetric air groove patterns in gold film on quartz substrates by optimizing the EBL and dry etching processes. The experimental demonstration of the applications of the structures is presented in Refs. 12 and 13. The paper is organized as follows. In Sec. 2, substrate preparation required before thin film deposition and lithography is presented. Section 3 presents the H-shape groove fabrication and Sec. 4 presents the optimized process for U-shaped grooves. Section 5 summarizes the results.

2 Substrate Preparation

Fabrication process involves degreasing the optically flat quartz substrates in vapors of trichloroethylene followed by acetone. To remove any residual liquid, we blow-dry the substrates with dry nitrogen gas and heat the substrates to 130°C for 8 min. A gold film of 100-nm thickness was deposited by sputtering on the quartz substrate. Initially, the chamber was evacuated to achieve 5×10^{-6} mbar pressure before introducing Argon gas of 30 sccm to have 8×10^{-3} mbar pressure during sputtering. A gold target of 99.99% purity was sputtered at 50 W rf-power for 4 min 40 s to achieve 100-nm-thick gold film. The thickness and surface quality of the gold film were tested by profilometer and AFM, respectively. Root-mean-square (rms) surface roughness of <1 nm was measured indicating very good quality deposition. The substrate with gold film was prebaked for 6 min at 175°C. For the required small feature sizes, we used ZEP520A-positive tone electron beam resist. The resist was spin coated on the gold film at 3000 rpm with a ramp of 300 rpm/s. The sample was then baked again for 6 min at 175°C to remove the residual solvent from the resist.

3 H-Shaped Air Holes in Gold Film

The computer aided design (CAD) was prepared for the plasmonic crystal structure with H-type air hole arrays. The period was chosen to be 300 nm with each vertical arm of the H-pattern to be 200-nm long and 50-nm wide. The horizontal arm connecting the two vertical arms is of 100-nm long and 50-nm wide. The design optimization is presented in Ref. 12. We used Raith e-Line EBL system. Although writing fine features, the dose at a given point is affected by that at the neighboring points. Thus, the dose calculation at each point has to be calculated properly by considering the effect of neighboring points and this is known as proximity error correction. We used the Nanopecs tool from Raith for proximity error correction to calculate the dose. To optimize the dose and other exposure conditions, we wrote 5×5 arrays of H-patterns initially. The accelerating voltage was 20 kV for the e-beam and to achieve fine features, we used 7.5-μm aperture. The exposed patterns are developed in ZED-N50 developer for 2 min followed by isopropyl alcohol (IPA) for 1 min which acts as a stopper. To transfer the pattern from resist to the gold, we use reactive ion etching. This involved two steps: in the first step, we etch gold using Argon plasma. To reduce the damage of gold film, we use 1-min etch stop for every 1 min etching. Different parameters are Argon mass flow 50 sccm, rf power 138 W, pressure of 1 Pa, and etch time was 7 min 20 s. To protect the ICP head of the Sentec SI 500 ICP-RIE system, we use a Teflon mask to cover the ICP head while doing metal etching. This is followed by oxygen plasma etching of the residual resist with oxygen mass flow 50 sccm, rf power 80 W, 1 Pa pressure, and etch time of 8 min. The steps involved in the fabrication process are shown in Fig. 1.

For dose optimization, we varied the dose from 100 to 600 μC/cm^2 in steps of 25. Although we found the pattern to be apple shaped with rounded off edges due to over exposure for dose >350 μC/cm^2, for dose >200 μC/cm^2, we did not find any pattern due to incomplete exposure

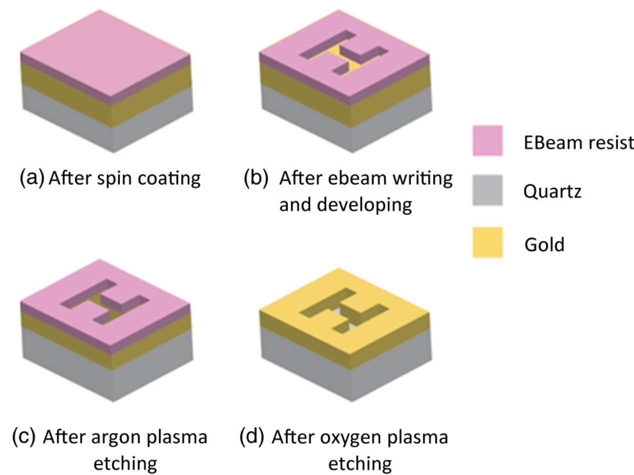

Fig. 1 Schematic of the fabrication process of H-slits in gold film is shown. The H-pattern has two-side channels or slits of rectangular shape as shown in (c). The slit is 50-nm wide and 200-nm long. The two-side channels are connected by a horizontal groove which is 50-nm wide and 100-nm long at the center. The required plasmonic metamaterial structure has periodicity of 300 nm to form a two-dimensional (2-D) array of H-patterns.

of the resist. So we optimized the resist thickness by thinning the resist by preparing a solution with two parts of ZEP520A and one part of Anisole (solvent of ZEP520A) by volume. This gave a resist thickness of 100 nm and for dose between 250 and 300 $\mu\text{C/cm}^2$, we could see the patterns transferred to gold after final etching. But still features were not sharp at the inner corners of H structure, where side channels and horizontal channel meet.

The CAD which used NanoPECS for proximity effect correction is shown in Fig. 2(a). The color code defines the dose at each point. For example, the dark blue region at the center has the smallest dose and the green color regions at the edges have the highest dose. The SEM image of the structure is shown in Fig. 2(b), which shows a distortion in the shape especially in the middle region where the dose is the largest.

To improve the fabrication, so that we realize a pattern close to the designed one, we tried different shapes in the CAD as shown in Figs. 3(a)–3(d). Figure 3(d) which shows the final CAD structure that gave the optimum pattern whose SEM image is shown. Initially, for the structure shown in Fig. 3(a), we obtained the desired structure in the dose range of 250 to 300. Successive improvisations made in the structure were (1) introducing the gaps between the side channels and central channel to reduce the proximity effect. The size of the gap was also varied and optimized, (2) changing the shape as well as the height and width of the central channel to reduce proximity effect. It can be seen that step-like features were introduced in the design to improve the structure. The idea was to have the central channel wide at the center and tapering toward the end to

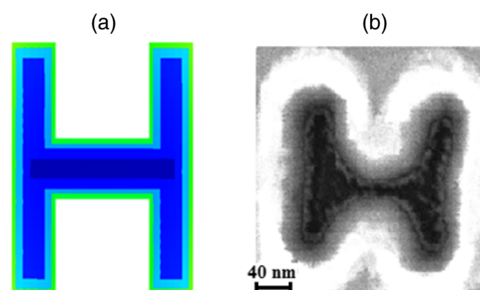

Fig. 2 (a) Initial CAD design of H-structure. (b) Corresponding SEM image obtained after electron beam lithography and reactive ion etching. Different dimensions are total width of H-pattern is 220.7 nm ($W = 200$ nm), length of the left arm is 193.7 nm ($L_l = 200$ nm), width of the left vertical arm is 79.04 nm ($W_l = 50$ nm), width of the right vertical arm is 84.08 nm ($W_r = 50$ nm), and width of the central arm is 68.65 nm ($W_c = 50$ nm). Numbers in brackets are designed values.

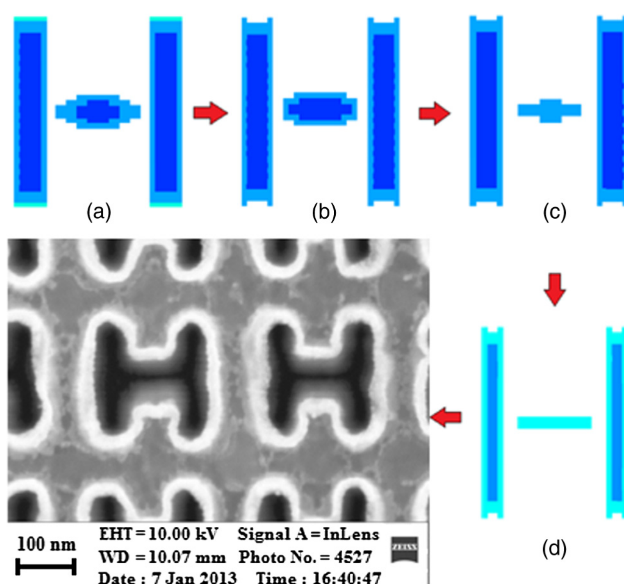

Fig. 3 Successive improvements tried in the CAD for H-pattern are shown in (a)–(c). (d) Final CAD of H-structure and the corresponding SEM image obtained after fabrication. Different dimensions are $W = 205.1$ nm (200 nm), $L_l = 198.5$ nm (200 nm), $W_l = 51.7$ nm (50 nm), $W_r = 50.54$ nm (50 nm), $W_c = 71.05$ nm (50 nm), and period = 295.2 nm (300 nm). Numbers in brackets are designed values.

counter the proximity effect at the edges, (3) height and width of the side channels were also varied to get required dimensions of the structure. Step-like features were introduced at the top and the bottom corners of the side channels to overcome the rounding effect at the edges, (4) adjusting various parameters of NanoPECS proximity error correction tool to get the final structure. One of the prominent parameter in NanoPECs is the step size. NanoPECS fragments the CAD into smaller pieces with minimum size of the fragment equal to the step size. The minimum step size in Raith e-Line EBL system is 2 nm. However, even with a step size of 6 nm, it took 7 h to write the pattern over 60×60 μm^2 area. Also, to write structures with dimensions <100 nm, we found that it gives correct features when we take all the dimensions of the structure in multiples of the step size. The final CAD, which was fragmented by NanoPECS with the step size of 6 nm, is shown in Fig. 4(a) after fragmenting. NanoPECS assigns dose to various fragments according to an algorithm based on proximity effect correction.

The final CAD, shown in Fig. 4(a), was assigned the dose pattern shown in Fig. 4(b). The dose variation is shown in terms of color coding. The color coding is assigned in terms of dose factor. Dose factor stands for the ratio of dose assigned for the fragment to base dose which was 250 $\mu C/cm^2$. Light blue color indicates the dose factor of 0.527 and the dark blue indicates a dose factor of 0.377. This design gave the final desired structure. The final structure was fabricated over an area of 60×60 μm^2. The optimum parameters are aperture size 7.5 μm, acceleration voltage 20 KV, 1000× magnification, 100 μm write-field, step size 0.006 μm, and base dose 250 $\mu C/cm^2$. Optical measurements demonstrated the proposed polarization switching between ~750- and ~1400-nm wavelengths.[12] A reasonably good match of the resonant wavelengths and the polarization switching mechanism shows that the obtained patterns are within acceptable error.[12]

4 U-Shaped Slits in Gold

Arrays of U-shaped slits are used to recently demonstrate the field localization and related bandpass filter application in THz-wavelength region.[13] Split-ring resonator structures are also fabricated by EBL for studies in THz-wavelength range. Initially, arrays of U-structures are

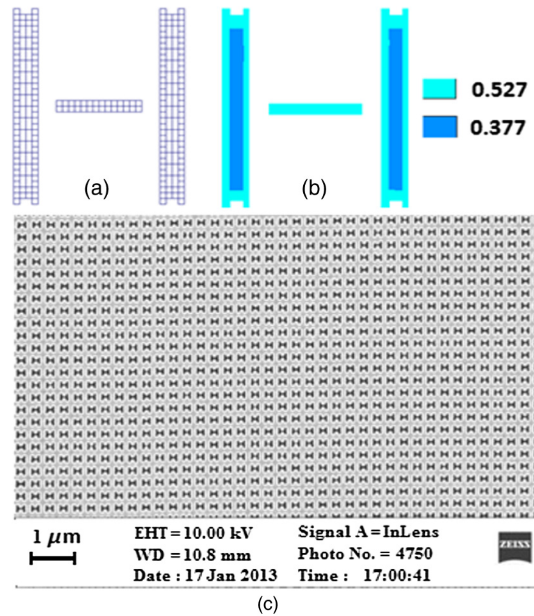

Fig. 4 (a) Final CAD that gave optimum H-pattern. (b) The dose variation within the pattern and (c) the SEM image of the final pattern written.

prepared. For THz-wavelength region, one would require large area patterns. The dimensions of the U-grooves to be written in gold film are shown in Fig. 5. To achieve the required large aspect ratio with EBL, we used a combination of fixed beam moving stage (FBMS) and normal writing. For example, to avoid stitching error while writing the long arm of the U, we need to use FBMS. However, as shown in Fig. 5, using a combination of FBMS areas resulted in not so good patterns. So, we used a combination of FBMS and normal area components. Two different combinations are used as shown in Fig. 5. Care must be taken while combining the FBMS and normal areas such that the alignment is perfect between them.

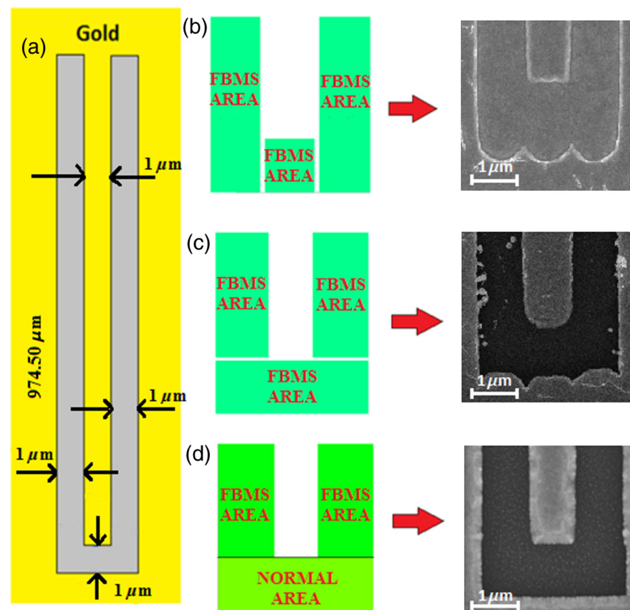

Fig. 5 Schematic of the U-shaped air groove which is to be written as a 2-D array in gold film. (b), (c), and (d) shows the different ways to write the pattern along with the SEM image of the pattern. Raster scanning of the e-beam dictates the final outcome of the pattern. A combination of FBMS and normal areas gave good results.

The final process for writing metamaterials for THz-wavelength range with U-shape constituents is a gold film of 100-nm thick that was deposited on clean fused silica substrate using rf-magnetron sputtering. E-beam resist PMMA 495A was spin coated on the gold layer at 2000 rpm with 400 ramp for 45 s and array of U aperture unit was written on the resist by EBL (Raith e-Line). The parameters such as aperture size (10 μm), write field ($100 \times 100\ \mu m^2$), and acceleration voltage (20 kV) were optimized to obtain the desired shape and size of the unit cell. After the exposure, the samples were developed in MIBK:IPA (1∶3) solution for 90 s at 21° C followed by rinsing in IPA for 60 s. Subsequently, the pattern was transferred onto the metal by reactive ion etching using Ar plasma. The following etch process parameters were set: etch time is 7 min 20 s, flow rate is 50 sccm, radiofrequency power is 138 W, and chamber pressure is 1 Pa. The residual resist was removed by oxygen etching process with the following parameters: etch time is 8 min, flow rate is 50 sccm, radiofrequency power is 80 W, and chamber pressure is 1 Pa. In the CAD, dose of FBMS and normal areas was varied from 100 to 250 $\mu C/cm^2$ in steps of 25 $\mu C/cm^2$ to find the optimum dose. In the final CAD, dose of 125 $\mu C/cm^2$ was given to FBMS areas and dose of 150 $\mu C/cm^2$ was given to normal areas. The normal areas were used at the top of the structure as well as at the bottom of the structure to get the desired result.

5 Conclusions

Large arrays of asymmetric shaped grooves in metal are interesting as they can be designed for various specific applications. Two structures are designed, one with H-shaped grooves for polarization-dependent switch at optical and near-infrared wavelengths and the second with U-shaped grooves for localizing THz radiation. These are high aspect ratio structures with the performance of the device critically dependent on the shape and uniformity of the structure. For precise writing of these patterns by EBL, the process was optimized in several steps. In addition to the standard parameters like the write-field, magnification, accelerating voltage, aperture size, proximity error correction among others, the CAD itself may need to be optimized to get the structure as close to the design as possible. We used FBMS method for stitch accuracy and also introduced etch stops to improve the gold surface quality after etching. We presented the optimization procedure used for two different patterns with large aspect ratios.

Acknowledgments

The authors would like to thank Prasanta Mandal and S.A. Ramakrishna for the H-pattern design.

References

1. W. L. Barnes, A. Dereux, and T. W. Ebbesen, "Surface plasmon subwavelength optics," *Nature* **424**(6950), 824–830 (2003), http://dx.doi.org/10.1038/nature01937.
2. K. Kneipp et al., "Single molecule detection using surface-enhanced Raman scattering (SERS)," *Phys. Rev. Lett.* **78**(9), 1667–1670 (1997), http://dx.doi.org/10.1103/PhysRevLett.78.1667.
3. B. Liedberg, C. Nylander, and I. Lundstrom, "Surface plasmon resonance for gas detection and biosensing," *Sens. Actuators* **4**(2), 299–304 (1983), http://dx.doi.org/10.1016/0250-6874(83)85036-7.
4. M.-K. Kwon et al., "Surface-plasmon-enhanced light-emitting diodes," *Adv. Mater.* **20**(7), 1253–1257 (2008), http://dx.doi.org/10.1002/(ISSN)1521-4095.
5. O. Stenzel et al., "Enhancement of the photovoltaic conversion efficiency of copper phthalocyanine thin film devices by incorporation of metal clusters," *Sol. Energy Mater. Sol. Cells* **37**(3–4), 337–348 (1995), http://dx.doi.org/10.1016/0927-0248(95)00027-5.
6. D. Derkacs et al., "Improved performance of amorphous silicon solar cells via scattering from surface plasmon polaritons in nearby metallic nanoparticles," *Appl. Phys. Lett.* **89**(9), 093103 (2006), http://dx.doi.org/10.1063/1.2336629.
7. V. I. Belotelov et al., "Plasmon-mediated magneto-optical transparency," *Nat. Commun.* **4**, 2128 (2013), http://dx.doi.org/10.1038/ncomms3128.

8. S. Kasture et al., "Strong coupling of in-plane propagating plasmon modes and their control," *Opt. Express* **21**(11), 13187–13192 (2013), http://dx.doi.org/10.1364/OE.21.013187.
9. P. Mandal et al., "Plasmon assisted intense blue-green emission from ZnO/ZnS nanocrystallites," *Opt. Mater.* **33**(11), 1786–1791 (2011), http://dx.doi.org/10.1016/j.optmat.2011.06.011.
10. V. I. Belotelov et al., "Enhanced magneto-optical effects in magnetoplasmonic crystals," *Nat. Nanotechnol.* **6**(6), 370–376 (2011), http://dx.doi.org/10.1038/nnano.2011.54.
11. S. Kasture et al., "Near dispersion-less surface plasmon polariton resonances at a metal-dielectric interface with patterned dielectric on top," *Appl. Phys. Lett.* **101**(9), 091602 (2012), http://dx.doi.org/10.1063/1.4749277.
12. P. Mandal et al., "Polarization dependent color switching by extra-ordinary transmission in H-slit plasmonic metasurface," *J. Appl. Phys.* **114**(22), 224303 (2013), http://dx.doi.org/10.1063/1.4842115.
13. R.-R. Lin et al., "Strong localization of terahertz wave and significant enhancement in electric field achieved in U-shaped resonators with a large aspect ratio," *Appl. Phys. Lett.* **103**(12), 123505 (2013), http://dx.doi.org/10.1063/1.4820809.
14. M. Rill et al., "Photonic metamaterials by direct laser writing and silver chemical vapour deposition," *Nat. Mater.* **7**(7), 543–546 (2008), http://dx.doi.org/10.1038/nmat2197.
15. S. Kawata et al., "Finer features for functional microdevices," *Nature* **412**(6848), 697–698 (2001), http://dx.doi.org/10.1038/35089130.
16. C. Enkrich et al., "Focused-ion-beam nanofabrication of near-infrared magnetic metamaterials," *Adv. Mater.* **17**(21), 2547–2549 (2005), http://dx.doi.org/10.1002/(ISSN)1521-4095.
17. S. Y. Chou, P. R. Krauss, and P. J. Renstrom, "Nanoimprint lithography," *J. Vac. Sci. Technol. B* **14**(6), 4129–4133 (1996), http://dx.doi.org/10.1116/1.588605.
18. N. Feth et al., "Large-area magnetic metamaterials via compact interference lithography," *Opt. Express* **15**(2), 501–507 (2007), http://dx.doi.org/10.1364/OE.15.000501.
19. J. Henzie, M. H. Lee, and T. W. Odom, "Multiscale patterning of plasmonic metamaterials," *Nat. Nanotechnol.* **2**(9), 549–554 (2007), http://dx.doi.org/10.1038/nnano.2007.252.
20. S. Zhang et al., "Experimental demonstration of near-infrared negative-index metamaterials," *Phys. Rev. Lett.* **95**(13), 137404 (2005), http://dx.doi.org/10.1103/PhysRevLett.95.137404.
21. T. Klimpel et al., "Model based hybrid proximity effect correction scheme combining dose modulation and shape adjustments," *J. Vac. Sci. Technol. B* **29**(6), 06F315 (2011), http://dx.doi.org/10.1116/1.3662879.
22. W. Zhang et al., "High-resolution electron beam lithography for the fabrication of high-density dielectric metamaterials," *Thin Solid Films* **515**(7–8), 3714–3717 (2007), http://dx.doi.org/10.1016/j.tsf.2006.09.011.
23. S. Kasture et al., "Proximity error correction method for continuous moving stage electron beam writing," *J. Vac. Sci. Technol. B* **30**(5), 050602 (2012), http://dx.doi.org/10.1116/1.4746259.

Raj Patil obtained his bachelor's degree in engineering from VIIT, Pune. He worked as a National Photonics Fellow at TIFR from June 2012 to May 2013. He is currently at University of Arizona where he is doing his masters in optical sciences.

Sheng Lan received PhD degree from Peking University, China. He was a postdoctoral fellow at NTU, Singapore (1995–1997) and Tuskuba University (1997–2000). He was a fellow in New Energy and Industrial Technology Development Organization, Japan (2000–2003) and a full professor at Shantou University. Since 2005, he is a professor in South China Normal University. He has more than 100 journal papers. His interests include nanophotonics, nonlinear and transient optics, and semiconductor materials and devices.

Achanta Venu Gopal received his PhD in physics from Solid State Electronics Group, TIFR, Mumbai and PhD in electronics from Tokyo University. He worked as a NEDO Fellow at FESTA Laboratories and as a JST Fellow at NEC Corporation, Tsukuba, Japan. In 2004, he joined TIFR where he is currently an associate professor. His research interests are in classical and quantum information processing and plasmonics. He has more than 65 journal publications. He is a Senior Member of IEEE and a member of OSA.